

WAVE PROCESSES IN THE SHOCK LAYER ON A FLAT PLATE AT AN ANGLE OF ATTACK

A. A. Maslov, S. G. Mironov, T. V. Poplavskaya, and I. S. Tsiryulnikov

UDC 532.526

A numerical and experimental study of receptivity of the viscous shock layer on a flat plate aligned at an angle of attack to external acoustic perturbations is performed. Density and pressure fluctuations are measured in experiments at the free-stream Mach number $M_\infty = 21$ and Reynolds number $Re_1 = 6 \cdot 10^5 \text{ m}^{-1}$. Direct numerical simulations of receptivity of the viscous shock layer to external acoustic perturbations in wide ranges of the governing parameters are performed by solving the Navier–Stokes equations with the use of high-order shock-capturing schemes. The calculated intensities of density and pressure fluctuations are found to be in good agreement with experimental data. Results of the study show that entropy-vortex disturbances dominate in the shock layer at small angles of attack, whereas acoustic perturbations prevail at angles of attack above 20° .

Key words: *hypersonic flows, shock layer, receptivity, direct numerical simulations, experiment.*

Introduction. A viscous shock layer is formed on the leading edges of hypersonic flying vehicles where the local Reynolds number is not too high and viscous forces prevail. The characteristics of disturbances in a hypersonic shock layer are determined by the following basic processes: action of free-stream perturbations on the shock layer, generation of disturbances inside the shock layer (receptivity), and evolution of disturbances during their downstream convection. These processes are interrelated, proceed simultaneously over the entire length of the shock layer, and can be defined as a unified process of distributed receptivity. Receptivity is an important characteristic of the initial stage of the laminar–turbulent transition. Acting on arising disturbances, one can control the laminar–turbulent transition in a high-velocity flow.

Previous experimental and numerical investigations of the characteristics of fluctuations generated by external acoustic waves in a hypersonic shock layer on a flat plate aligned at a zero angle of attack [1] showed that the main features of the formation of the field of density fluctuations are generation of entropy-vortex disturbances and their domination inside the shock layer. Interacting with the mean flow, these disturbances form the field of density fluctuations. In particular, there are two peaks of density fluctuations: on the shock wave (SW) and on the boundary-layer (BL) edge where the mean density gradient reaches high values. Vortices propagate in the inviscid layer between the SW and the BL edge. It was also demonstrated [1, 2] that the role of the acoustic mode of disturbances is enhanced as the angle between the direction of external acoustic disturbances and the SW increases.

Subsequent experimental and numerical studies [2] made it possible to supplement and refine the characteristics of the entropy-vortex mode disturbances developed in the shock layer on a flat plate at a zero angle of attack. It was shown that specific features of these disturbances are the coincidence of the spatial distributions of fluctuations in the shock layer and the equality of the streamwise phase velocities of disturbances regardless of the source of their generation. For this reason, an interference pattern of controlling the disturbance intensity in a hypersonic shock layer on a flat plate could be realized in experiments and numerical simulations [3].

Khristianovich Institute of Theoretical and Applied Mechanics, Siberian Division, Russian Academy of Sciences, Novosibirsk 630090. Novosibirsk State University, Novosibirsk 630090; maslov@itam.nsc.ru; mironov@itam.nsc.ru; popla@itam.nsc.ru; tsivan@ngs.ru. Translated from *Prikladnaya Mekhanika i Tekhnicheskaya Fizika*, Vol. 51, No. 4, pp. 39–47, July–August, 2010. Original article submitted March 29, 2010.

At the same time, the surface of a real hypersonic flying vehicle contains some areas aligned at a non-zero angle of attack. On these areas, the angle of SW inclination to the free-stream direction and the angle of incidence of external perturbations onto the SW increase, and the distributions of flow parameters in the shock layer become different. It follows from [4] that the modal composition of disturbances arising behind the SW due to its interaction with acoustic waves in the incoming flow depends substantially on the angle of incidence of acoustic waves onto the SW. In particular, the fraction of acoustic disturbances rapidly increases with increasing angle of incidence. Interacting with the surface and with the SW, acoustic disturbances generate a complicated pattern of pressure, density, and temperature fluctuations in the shock layer, which is superimposed onto the field of fluctuations formed by the entropy-vortex mode of disturbances. It was also shown [3] that the emergence of acoustic disturbances in the shock layer decreases the efficiency of the interference control of disturbances with the use of a local blowing–suction source. Therefore, it is of interest to study the receptivity and evolution of disturbances in a hypersonic shock layer on a flat plate aligned at an angle of attack under the action of external acoustic waves on this layer.

The present paper describes the results of a comprehensive numerical and experimental study of distributed receptivity of a hypersonic shock layer on a flat plate mounted at an angle of attack α to free-stream acoustic disturbances. The behavior of density and pressure fluctuations in the shock layer on the flat plate is studied as a function of the angle of attack with variations of the frequency of external acoustic waves and the angle of incidence of disturbances onto the SW.

Experimental Equipment and Measurement Technique. The experiments were performed in a T-327A hypersonic nitrogen wind tunnel based at the Khristianovich Institute of Theoretical and Applied Mechanics of the Siberian Division of the Russian Academy of Sciences. The following test conditions were used: free-stream Mach number $M_\infty = 21$, unit Reynolds number $Re_{1\infty} = 6 \cdot 10^5 \text{ m}^{-1}$, angles of attack on the windward side of the plate $\alpha = 0\text{--}30^\circ$, stagnation temperature $T_0 = 1200 \text{ K}$, and surface (wall) temperature $T_w = 300 \text{ K}$.

The experiments were performed with a steel plate of length $L = 110 \text{ mm}$ and thickness 25 mm ; the width of the leading and trailing edges was 50 mm . The wedge angles were 30° (for the leading edge) and 75° (for the side edges). The streamwise and spanwise sizes of the flat plate were determined by the maximum admissible blockage of the flow by the model mounted at an angle of attack $\alpha = 30^\circ$, with the minimum influence of the side edges on the flow at the plate centerline. The angle of attack of the flat plate was changed by an electric motor; the accuracy of the angle of attack was monitored by a circular slide wire. In some experiments, an I4301 pressure sensor 4 mm in diameter was flush-mounted with the plate surface on the plate centerline at a distance of 100 mm from the leading edge. In electron-beam measurements, the pressure sensor was replaced by a graphite insert $15 \times 15 \text{ mm}$ to suppress secondary electron emission from the diagnosing electron beam.

The parameters measured in the experiments were the pressure fluctuations on the plate surface and also the distributions of the mean density and density fluctuations normal to the surface at discrete points along the plate centerline. The pressure fluctuations were measured by a piezoceramic sensor, and the distributions of the mean density and density fluctuations were measured by the method of the electron-beam fluorescence [5]. The procedure of reconstruction of the mean density and the field of density fluctuations from the fluorescence signal was described in [2]. The fluctuations were measured in the frequency range from 3 to 50 kHz . Electron-beam visualization of the flow was performed to obtain the overall pattern of the flow past the plate.

Numerical Method. A hypersonic flow ($M_\infty = 21$) past a flat plate aligned at an angle of attack with a viscous shock layer formed over the entire plate length, which is characterized by a strong viscous-inviscid interaction, was studied in this work. The hypersonic flow theory [6] involves an interaction parameter $\chi = M_\infty^3 / \sqrt{Re_x}$, which characterizes the degree of the viscous-inviscid interaction. Two flow regimes are distinguished, depending on the value of this parameter: strong viscous-inviscid interaction at $\chi > 1$ and weak viscous-inviscid interaction at $\chi < 1$. In our study, the values $\chi = 84.5, 59.8, 48.8, 42.3,$ and 37.8 were obtained in the flow past a flat plate 100 mm long at the streamwise coordinates $x/L = 0.2, 0.4, 0.6, 0.8,$ and 1.0 , respectively. Thus, the regime of a strong viscous-inviscid interaction corresponding to high-Mach-number flows is formed in the entire flow past the plate in the case considered.

The most unstable disturbances in boundary layers at high Mach numbers are known to be those that propagate at a zero angle to the main flow direction [7]. This means that the flow remains two-dimensional at the early stages of the transition to turbulence. Experiments performed at the Mach number $M_\infty = 21$ [1, 3] also showed that two-dimensional waves prevail both in the free stream and in the shock layer on the flat plate.

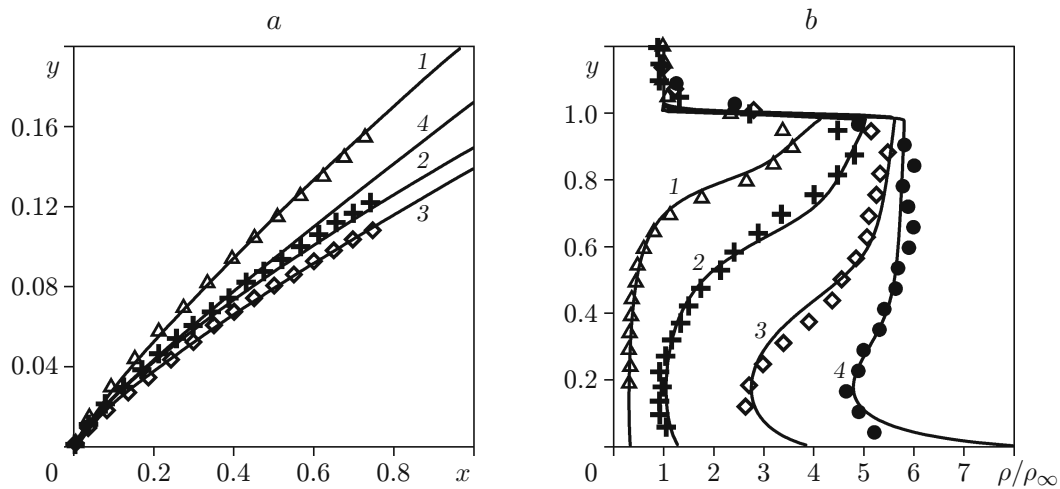


Fig. 1. SW location (a) and mean density profiles (b) in the cross section $x = 0.95$ obtained in the experiment (points) and calculations (solid curves) at $M_\infty = 21$, $Re_L = 6 \cdot 10^4$, $T_w = 300$ K, $T_0 = 1200$ K, and different angles of attack: $\alpha = 0$ (1), 10 (2), 20 (3), and 30° (4).

Therefore, two-dimensional Navier–Stokes equations with high-order shock-capturing schemes [8] are solved in the present work in direct numerical simulations of the evolution of disturbances. The numerical method is described in detail in [1].

The computational domain is a rectangle; part of its lower side coincides with the plate surface. The left (input) boundary is located at a distance equal to the length of several computational cells upstream from the leading edge of the plate. The height of the computational domain is chosen in a manner to avoid interaction of the bow SW propagating from the leading edge with the upper boundary. The right (output) boundary is shifted away from the trailing edge of the plate, so that the flow in the output section is completely supersonic.

First, we performed steady flow calculations, with a uniform hypersonic flow being specified on the left and upper boundaries. The solution on the right boundary was extrapolated from inside the computational domain. Velocity slip and temperature jump were taken into account in the boundary conditions. Conditions of symmetry were set on the other part of the lower boundary (which did not coincide with the plate surface).

In solving the problem of interaction of the viscous shock layer with external acoustic waves, the variables on the left boundary of the computational domain were defined in the form of a superposition of the steady main flow and a plane monochromatic acoustic wave characterized by the amplitude A , propagation angle θ , and frequency f . The same boundary conditions that were used to find a steady solution were also applied on the plate surface, with the only exception that temperature disturbances on the surface were assumed to be equal to zero: $T'|_{y=0} = 0$ (by virtue of significant thermal inertia of the plate). After introduction of disturbances, the Navier–Stokes equations were integrated until the unsteady solution reached a stationary periodic regime.

A uniform computational grid with the x step of 0.0009 and the y step of 0.0005 was used. The computational program was parallelized with the use of the MPI library, which allowed our computations to be performed on multiprocessor computers. Up to 20 processors of the Siberian Supercomputer Center (Novosibirsk) were used in the computations.

It was demonstrated in [1–3], where the flow in a hypersonic shock layer on a flat plate aligned at a zero angle of attack was considered, that this algorithm and calculation method can be used to solve problems of BL receptivity and stability.

Results. In the present work, the flow was visualized by an electron beam at the angles of attack $\alpha = 0$, 10 , 20 , and 30° to determine the SW position and the ranges of SW angles with respect to the flow direction for each angle α . A comparison of the visualization results with the calculated density fields for a steady flow revealed their good agreement.

Figure 1 shows the experimentally measured and calculated SW positions (Fig. 1a) and the mean density profiles in the cross section $x = 0.95$ (Fig. 1b) for different angles of attack of the flat plate. It is seen that the

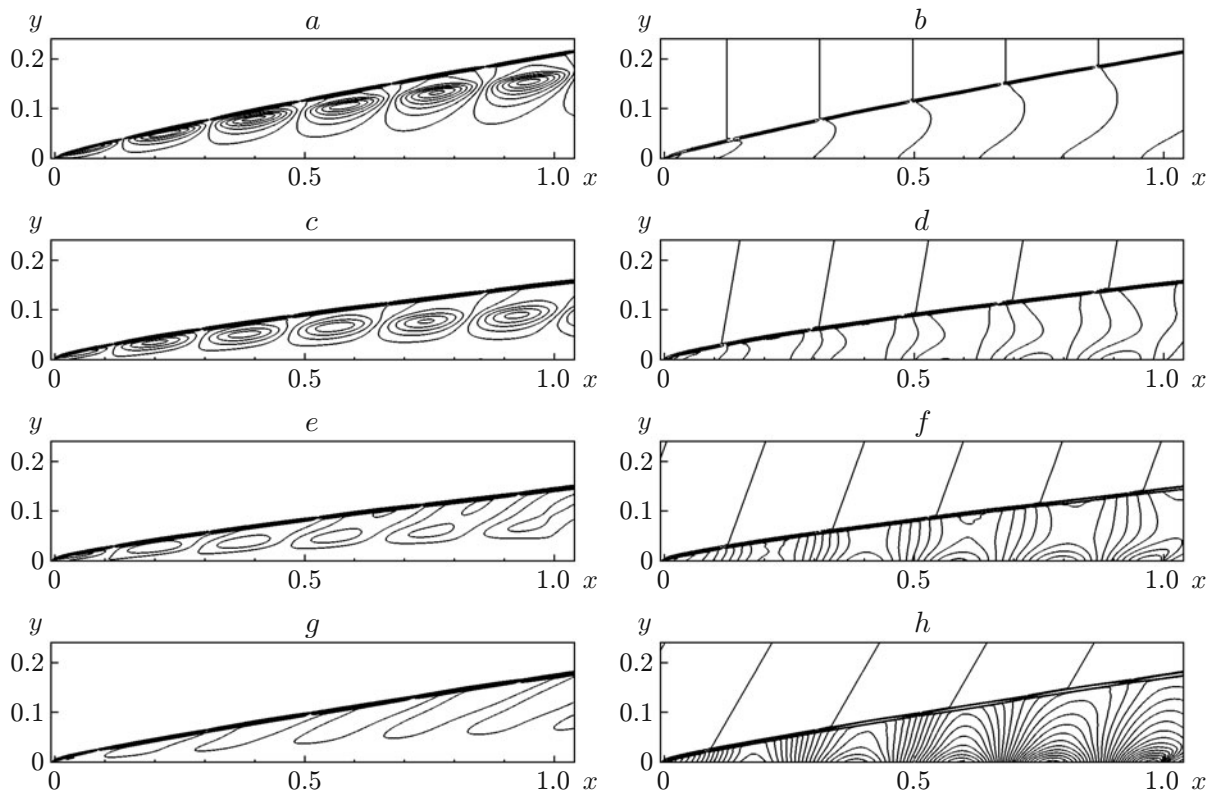


Fig. 2. Calculated flow fields of entropy fluctuations (a, c, e, and g) and pressure fluctuations (b, d, f, and h) in the shock layer for different angles of attack: $\alpha = 0$ (a and b), 10° (c and d), 20° (e and f), and 30° (g and h).

calculated and experimental values are in good agreement. As the angle of attack is increased to $\alpha = 20^\circ$, the SW becomes pressed to the plate surface, whereas the SW detachment is observed at $\alpha > 20^\circ$. The BL thickness (low-density areas in Fig. 1b) substantially decreases thereby. The less steep slope of the measured profile of density on the SW is apparently caused by significant SW oscillations in the experiment and by the limited resolution of the measurement equipment. As a whole, the numerical algorithm ensures a fairly accurate description of the mean flow in the shock layer.

Figure 2 shows the calculated fields of entropy and pressure fluctuations in the shock layer for different angles of attack. It is seen that the fraction of entropy-vortex disturbances behind the SW drastically decreases with increasing angle of attack α , while pressure fluctuations increase, with the most intense growth of pressure fluctuations being observed on the plate surface. The maximum intensity of pressure fluctuations on the plate surface is observed in the hypersonic boundary layer at Mach numbers $M_\infty < 10$ [9–11], at which acoustic disturbances prevail.

The result of direct numerical simulations agree with the results calculated by the linear theory of interaction of disturbances with the SW [4]. Following [4], we calculated the domains of existence of disturbances of various modes in the shock layer for the test conditions used. It was found that entropy-vortex disturbances dominate in the shock layer at $M_\infty = 21$ and $\alpha = 0$ and 10° , while acoustic waves exponentially decay; at angles of attack $\alpha \geq 20^\circ$, non-decaying acoustic disturbances arise in the shock layer in addition to entropy-vortex disturbances.

Figure 3 shows the profiles of density fluctuations in the cross section $x = 0.95$, which were obtained in the calculation and experiment at different angles of attack. It is seen that the calculated and experimental results are in good agreement.

Figure 4 shows the calculated profiles of pressure and entropy fluctuations in the same cross section $x = 0.95$. At $\alpha = 0$ and 10° , there are peaks of density (see Figs. 3a and 3b) and entropy (Fig. 4b) fluctuations in the shock layer on the BL edge, which are induced by interaction of vortex disturbances with the mean flow [1]. At $\alpha = 20$ and 30° , density fluctuations (see Figs. 3c and 3d) do not display a clearly expressed local maximum on the BL edge;

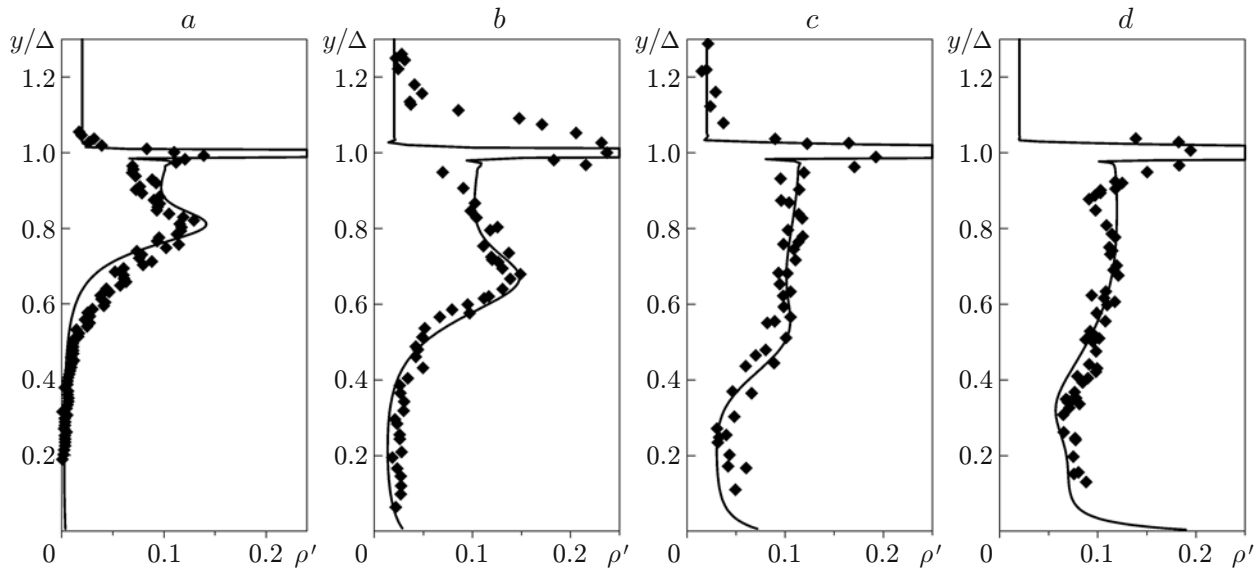


Fig. 3. Profiles of density fluctuations ρ' in the cross section $x = 0.95$ obtained in the calculations (solid curves) and experiment (points) at $M_\infty = 21$, $Re_L = 6 \cdot 10^4$, $A = 0.03$, and $f = 30$ kHz: (a) $\alpha = 0^\circ$ and $\theta = 0^\circ$; (b) $\alpha = 10^\circ$ and $\theta = 10^\circ$; (c) $\alpha = 20^\circ$ and $\theta = 20^\circ$; (d) $\alpha = 30^\circ$ and $\theta = 30^\circ$.

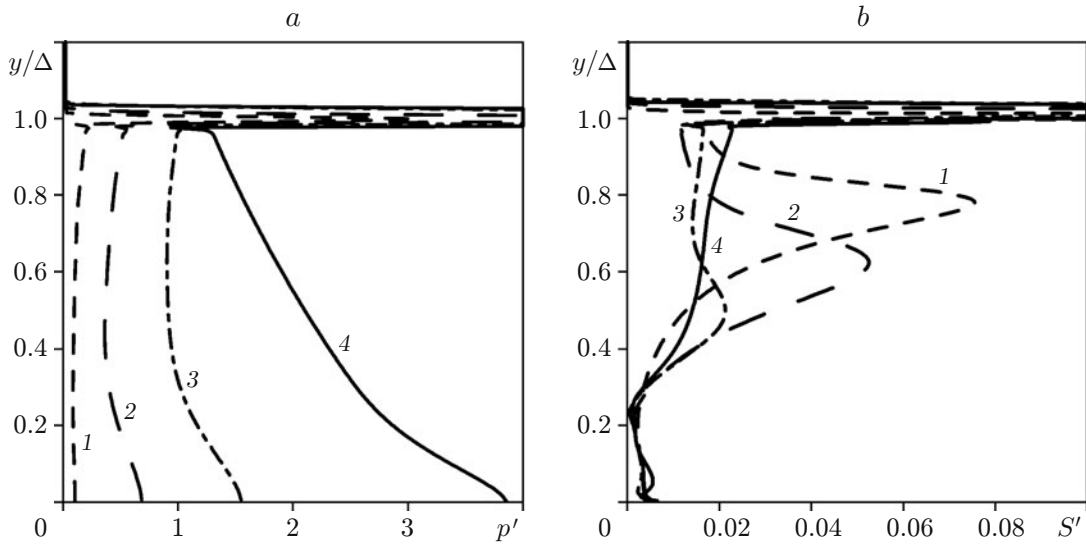


Fig. 4. Profiles of pressure fluctuations p' (a) and entropy fluctuations S' (b) in the cross section $x = 0.95$ at $M_\infty = 21$, $Re_L = 6 \cdot 10^4$, $A = 0.03$, and $f = 30$ kHz: $\alpha = 0^\circ$ and $\theta = 0^\circ$ (1), $\alpha = 10^\circ$ and $\theta = 10^\circ$ (2), $\alpha = 20^\circ$ and $\theta = 20^\circ$ (3), and $\alpha = 30^\circ$ and $\theta = 30^\circ$ (4).

moreover, the intensity of disturbances near the plate surface is greater than the corresponding values obtained at small angles of attack. As the angle of attack α is increased, it is seen that the entropy fluctuations behind the SW decrease, whereas the pressure fluctuations p' increase. The growth of pressure fluctuations is apparently caused by the increase in the fraction of acoustic disturbances; the most significant increase is observed at $\alpha = 20$ and 30° , which agrees with the estimates obtained by the theory of interaction of disturbances with the SW [4]. It follows from Figs. 3 and 4 that the BL receptivity is qualitatively different at small and large angles of attack. Density fluctuations are determined by non-acoustic disturbances at small angles of attack α , but the sources of density fluctuations at large values of α are both non-acoustic and acoustic disturbances.

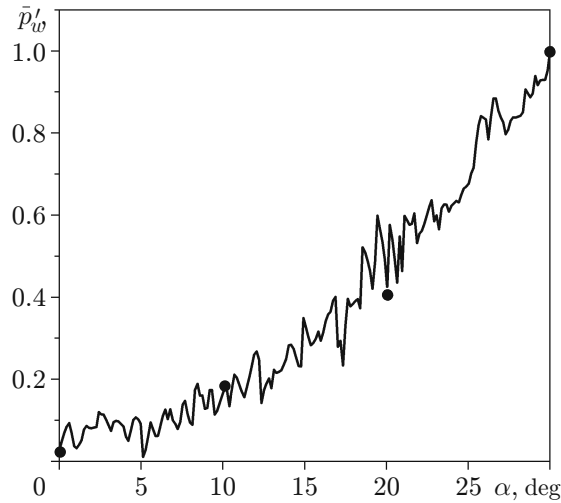


Fig. 5. Normalized spectral amplitude of pressure fluctuations versus the angle of attack of the flat plate at $M_\infty = 21$, $Re_L = 6 \cdot 10^4$, $A = 0.03$, and $f = 30$ kHz: the solid curve and the points show the experimental and calculated results, respectively.

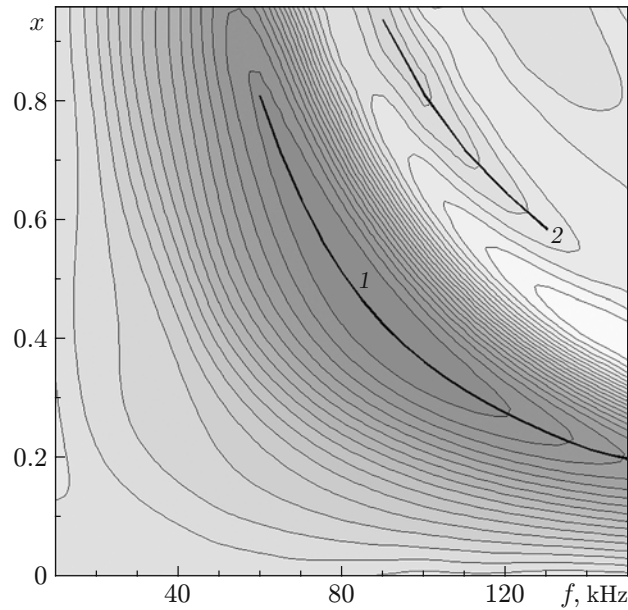


Fig. 6. Isolines of the amplitude of pressure fluctuations in the plane (f, x) at $M_\infty = 21$, $Re_L = 6 \cdot 10^4$, $A = 0.03$, and $\alpha = 30^\circ$: curves 1 and 2 show the maximums of pressure fluctuations.

As was demonstrated above, the most intense growth of pressure fluctuations in the shock layer at different angles of attack is observed on the plate surface (see Fig. 2b). Therefore, the intensity of acoustic disturbances in the experiment is determined with the use of sensors of pressure fluctuations on the model surface. The results of these measurements for the frequency $f = 30$ kHz are plotted in Fig. 5 as the amplitude of pressure fluctuations \bar{p}'_w versus the angle of attack α continuously changed from 0 to 30° . The amplitude of pressure fluctuations is normalized to its value at $\alpha = 30^\circ$ ($\bar{p}'_w = p'_w/p'_w|_{\alpha=30^\circ}$). Similar dependences were obtained for all frequencies of pressure fluctuations. In the experiment at small angles of attack, the pressure fluctuations were also small; for this reason, the relative error of determining their values was rather large. Nevertheless, a comparison of the measured dependence with the numerical results (points in Fig. 5) shows their good agreement.

The amplitude of pressure fluctuations on the plate surface was studied numerically as a function of frequency and streamwise coordinate at $\alpha = 30^\circ$. Figure 6 shows the calculated results in the form of the amplitude isolines of pressure fluctuations p'_w . It is seen that the amplitude of pressure fluctuations at any frequency has a maximum at points with certain streamwise coordinates x . The diagram shows two areas with a significant intensity of pressure fluctuations p'_w ; the locations of the maximums of these areas is shown by curves 1 and 2. Thus, the intensity of pressure fluctuations in the shock layer increases in the downstream direction in the examined range of wavelengths of external disturbances. At $\alpha = 30^\circ$, the Mach number behind the SW is $M \approx 4$. Therefore, the dependences in Fig. 6 are similar to those obtained for disturbances in the BL on the flat plate at $\alpha = 0^\circ$ and the Mach number on the BL edge $M = 4$ [12].

Conclusions. The paper describes the results of a numerical and experimental study of receptivity of a viscous shock layer on a flat plate to external acoustic waves for different angles of attack of the plate. Specific features of interaction of acoustic disturbances with the viscous shock layer are studied in a wide range of frequencies. As the angle of attack is increased, the shock-layer and boundary-layer thicknesses are shown to decrease, whereas the intensity of pressure fluctuations increases. In particular, intense acoustic waves are generated behind the SW at the angles of attack $\alpha > 20^\circ$, whereas intense non-acoustic disturbances are observed at $\alpha < 20^\circ$. This result agrees with the predictions by the inviscid linear theory of SW–disturbance interaction. A range of wavelengths of external disturbances with downstream enhancement of the intensity of pressure fluctuations in the shock layer is found to exist.

The authors are grateful to A. N. Kudryavtsev for the program used to solve the Navier–Stokes equations and useful discussions.

This work was performed within the framework of the Analytical Departmental Targeted Program No. 2.1.1/3963 entitled “Development of the Scientific Potential of the Higher School” and was also supported by the Russian Foundation for Basic Research (Grant No. 09-08-00557).

REFERENCES

1. A. N. Kudryavtsev, S. G. Mironov, T. V. Poplavskaya, and I. S. Tsyryulnikov, “Experimental study and direct numerical simulation of the evolution of disturbances in a viscous shock layer on a flat plate,” *J. Appl. Mech. Tech. Phys.*, **47**, No. 5, 617–627 (2006).
2. A. A. Maslov, A. N. Kudryavtsev, S. G. Mironov, et al., “Numerical simulation of receptivity of a hypersonic boundary layer to acoustic disturbances,” *J. Appl. Mech. Tech. Phys.*, **48**, No. 3, 368–374 (2007).
3. A. A. Maslov, A. N. Kudryavtsev, S. G. Mironov, et al., “Control of disturbances in a hypersonic shock layer on a flat plate by an unsteady action from the surface,” *Izv. Ross. Akad. Nauk*, No. 3, 152–161 (2008).
4. J. F. McKenzie and K. O. Westphal, “Interaction of linear waves with oblique shock waves,” *Phys. Fluids*, **11**, 2350–2362 (1968).
5. S. G. Mironov and A. A. Maslov, “An experimental study of density waves in hypersonic shock layer on a flat plate,” *Phys. Fluids*, **12**, No. 6, 1544–1553 (2000).
6. W. D. Hayes and R. F. Probstein, *Hypersonic Flow Theory*, Academic Press, New York (1959).
7. S. A. Gaponov and A. A. Maslov, *Development of Disturbances in Compressible Flows* [in Russian], Nauka, Novosibirsk (1980).
8. A. N. Kudryavtsev, T. V. Poplavskaya, and D. V. Khotyanovskii, “Application of high-order schemes in modeling unsteady supersonic flows,” *Mat. Model.*, **19**, No. 7, 39–55 (2007).
9. X. Zhong, “Receptivity of hypersonic boundary layers to freestream disturbances,” AIAA Paper No. 2000-0531 (2000).
10. I. V. Egorov, V. G. Soudakov, and A. V. Fedorov, “Numerical simulation of receptivity of a supersonic boundary layer to acoustic disturbances,” *Izv. Ross. Akad. Nauk, Mekh. Zhidk. Gaza*, No. 1, 42–53 (2006).
11. I. V. Egorov, A. V. Fedorov, and V. G. Soudakov, “Receptivity of a hypersonic boundary layer over a flat plate with a porous coating,” *J. Fluid Mech.*, **601**, 165–187 (2008).
12. L. M. Mack, “Linear stability theory and the problem of supersonic boundary-layer transition,” *AIAA J.*, **13**, No. 3, 278–289 (1975).